Small scale sCO_2 compressor impeller design considering real fluid conditions

S. Schuster, F.-K. Benra, D. Brillert

Abstract

Supercritical carbon dioxide cycles are extremely compact and hence offer a new and a wide range of applications. Besides the benefits of a compact cycle some challenges arise for the turbo machinery development. In this paper a first design for the compressor applied to the Brayton cycle is presented. The Brayton cycle is used for the supercritical heat removal system (sCO2-HeRo) which safely removes residual heat from a nuclear power plant (Venker et al., 2010, 2014). Based on the sCO2-HeRo system the design procedure for the compressor is explained and the implementation of the real fluid properties into the CFD code is reviewed. Finally, the influence of the real fluid properties on the aerodynamic performance is discussed.

Nomenclature

a	Specific work
c_p	Isobaric heat capacity
$c_{u,1}$	Swirl velocity component at impeller inlet
$c_{u,2}$	Swirl velocity component at impeller outlet
d_2	Impeller outlet diameter
$\dot{m}$	Mass flow
n	Rotational speed
n_{Blade}	Number of blades
P_{is}	Isentropic power
p_{tot}	Total pressure
T_{tot}	Total temperature
u_1	Circumferential velocity at impeller inlet
u_2	Circumferential velocity at impeller outlet
$\dot{V}$	Volume flow
z	Number of impeller blades
φ	Flow coefficient
ρ	Density
λ	Heat conductivity
η	Dynamic viscosity

Introduction

Brayton cycles are utilized since many years for electricity generation. Very often the thermodynamic process is realized in an open gas turbine process. In such processes air is taken in and compressed in a multistage axial compressor. Thereafter, fuel is injected, mixed with the air and the mixture is ignited. The hot gas propels a turbine that drives the compressor and a second turbine that converts the thermal energy into

mechanical work. The mechanical work is used to drive a generator or even a machine which takes the work for powering. The described process is characterized by a high volume flow of the working fluid which documents the need for big machines. In contrast to the open gas turbine cycle the turbomachinery components for sCO_2 Brayton cycles are small, even though the concept is the same. The sCO_2 Brayton cycle is a closed gas turbine process consisting of a compressor, external heat source, a turbine and external heat sink. Due to the high density and high heat capacity of the working fluid, the volume flow in sCO_2 Brayton cycles is several magnitudes lower compared to the classic Brayton cycle operating with air and exhaust gas. At the compressor inlet the density of the fluid is 500 times higher compared to the open gas turbine process working with air. The heat capacity at the compressor inlet is 25 times higher than that of an open Brayton cycle. Even though very small cycles can be realized having a high power output, the components of those small cycles are quite small leading to diverse challenges during the design process. This becomes even more important for demonstrators, as these are smaller compared to the implemented systems. Besides the possibility to provide surplus energy, Brayton cycles can also be used for heat transfer from a hotter side to a colder side and can work self-propellant. Such a system can be used for emergency cooling and is independent from external energy sources. Therefore, the system is favorable for being an additional emergency system in a nuclear power plant. The turbomachine presented in this paper is designed exactly for this purpose. Nevertheless presented results have a general meaning and can be adopted for other fields of application. The overall system is presented by Benra et al. (2016) and only the parts directly linked to this paper will be presented in the following.

The concept of the emergency system is already formulated and presented by Venker (2010, 2014). The next step is to prove the concept in a small scale demonstrator. Therefore, the so called glass model located at GfS Simulatorschule in Essen, Germany is utilized. The glass model is a small scale version of a pressurized water reactor with an electrical heated core. Several off-design accident cases can be demonstrated in the glass model. The sCO2-HeRo system will be implemented into the glass model which makes it possible to show which accident cases can be avoided if the sCO2-HeRo is established.

The available heat for the demonstrator is 200 kW at a maximum temperature of 200 °C. Compared to the decay heat in nuclear power plants (50 MW), the available heat for the demonstrator is several magnitudes lower. Even though the 50 MW sCO2-HeRo system is quite small, the demonstrator is much smaller and hence provides a challenge in terms of size. Small volume flows require high rotational speeds to achieve good turbomachinery efficiencies (Aungier, 2000). However the rotational speed is limited by mechanical constraints. Furthermore, the frictional losses get extraordinarily high with increasing rotational speed. This is mainly a reason of the encapsulated system. Besides the size, the large change of fluid properties at very small pressure differences will be a big challenge for the compressor design.

In this paper an initial compressor design for the sCO2-HeRo system is presented. The efficiency obtained from a CFD simulation and the power needed to drive the compressor is given. Calculations with real fluid properties and constant fluid properties are conducted to show the influence of changing fluid properties on the flow in the compressor.

Design

The decay heat in nuclear power plants is 5% of the nominal power output shortly after shutdown and stays constant for almost 72 hours. For the sCO2-HeRo system this means that 50 MW heat must be transferred from the reactor core to the alternative ultimate heat sink. This situation results in large components for the heat removal system. For the demonstrator the available heat is only 200 kW and hence the heat removal components are much smaller. The temperature of the fluid in the steam generator and the temperature of the ultimate heat sink are equal for the demonstrator and the implemented system. As a consequence, the sCO_2 mass flow is smaller in the demonstrator compared to the implemented system. The mass flow ratio and the ratio of decay heat between both the systems are equal.

In order to compare both systems the pressure ratios of compressor and turbine as well as the temperatures are kept the same. With assumed component efficiency the specific work can be calculated.

From the Euler equation the specific work can be obtained with Eq. 1 for the case that radially oriented blades are used. Either rotational speed n or outlet diameter d_2 must be specified, in order to calculate the other parameter. To compute one of the parameters, more information is needed and therefore, the flow coefficient φ, on which the efficiency depends, is used. Flow coefficient is defined by Eq. 2, the efficiency as a function of this coefficient is given by Aungier (Aungier, 2000). The best efficiency can be expected at a flow coefficient of 0.1. This requires a rotational speed of 160,000 rpm. Such a high value of the rotational speed causes large frictional losses. Therefore, the rotational speed must be limited to 50,000 rpm resulting in a slightly lower flow coefficient and efficiency. In Tab. 1 the design parameters of the compressor are given.

$$a = u_2 \cdot c_{u,2} - u_1 \cdot c_{u,1} = u_2 \cdot c_{u,2} = u_2^2 = \left(\pi \cdot n \cdot d_2\right)^2 \text{ (no swirl at the inlet } c_{u,1} = 0) \quad (1)$$

$$\varphi = \frac{4 \cdot \dot{V}}{\pi \cdot d_2^2 \cdot u_2} = \frac{4 \cdot \pi \cdot \dot{V}}{a^{3/2}} n^2 \quad (2)$$

Rotational speed / rpm	n	50,000	rpm
Number of impeller blades	n_{Blade}	22	
Mass flow	$\dot{m}$	0.65	kg/s
Isentropic Power	P_{is}	5.046	kW
Impeller outlet diameter	d_2	40	mm

Table 1 – Design parameters

The parameters given in Tab. 1 are the initial point for a detailed design of the impeller. Further considerations must be applied to draw the mean line and the thickness distribution of the blades. These parameters are given in chapter “Aerodynamics of sCO2_HeRo_CC_1002”

Aerodynamic analysis

CFD-code

The results presented in the chapter “Real fluid properties” and “Aerodynamics of sCO2_HeRo_CC_1002” are based upon solutions of the Reynolds-Averaged-Navier-Stokes equations. With the finite volume method the partial differential equations are transformed into an algebraic set of equations which can be solved using a CFD program. Ansys CFX is used for the described procedure. Menter´s SST model has been used as the turbulence model for the simulations (Menter, 1994).

Real fluid properties

Near the critical point of carbon dioxide small changes in pressure result in large density variations. Therefore, incorporation of sophisticated real fluid properties must be taken into consideration. For the CFD analysis real fluid data is provided as tabulated values. The properties of the real fluid are taken from a fluid property library (Kretzschmar, 2014). The resolution of the tabulated properties influences significantly the speed of the CFD code. Therefore the necessary resolution of the table steps is investigated by performing calculations in a straight tube. Starting from a very coarse resolution of 10 pressure values x 10 temperature values the resolution is increased up to 400 x 400. The lower pressure is 74 bar, the upper pressure is 145 bar, the lower temperature is 304.15 K and the upper temperature 393.15 K. Steady state calculations of the flow are performed with a discretization of second order accuracy in space in a tube of 0.01 m radius and 0.1 m length. For the boundary conditions at the inlet, the total pressure and the total temperature are specified and the boundary condition at the outlet is the mass flow rate. The spatial mesh is given by 60 nodes in radial direction, 3 nodes in circumferential direction and 100 nodes in axial direction.

In Fig. 1 the density ρ and the isobaric heat capacity c_p are plotted as a function of the table resolution. CFD results are highlighted with symbols connected with lines. Black line and circles are showing the density ρ, red line with “X” mark shows the isobaric heat capacity c_p. With increasing table resolution the obtained values are converging against a threshold value. This threshold is close to the values which can be obtained by the direct calculation of properties with the Equation of State (EOS) as can be seen from Fig. 2. To calculate the fluid properties with the EOS, pressure and temperature are taken from the CFD simulation as an input.

In Fig. 2 the error is shown for different fluid properties: ρ – density, c_p specific heat capacity, η dynamic viscosity, λ heat conductivity. The conformity between numerical and EOS values is satisfactory for a number of 40,000 tablepoints.

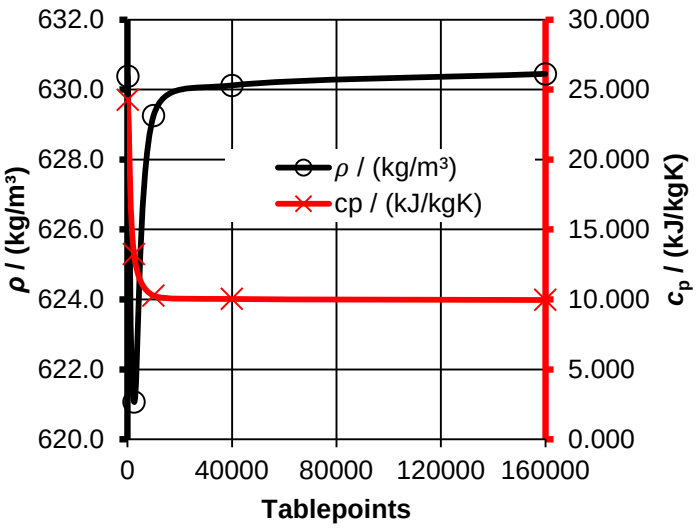

Figure 1 – Independency of the calculated values for ρ and c_p from the table resolution

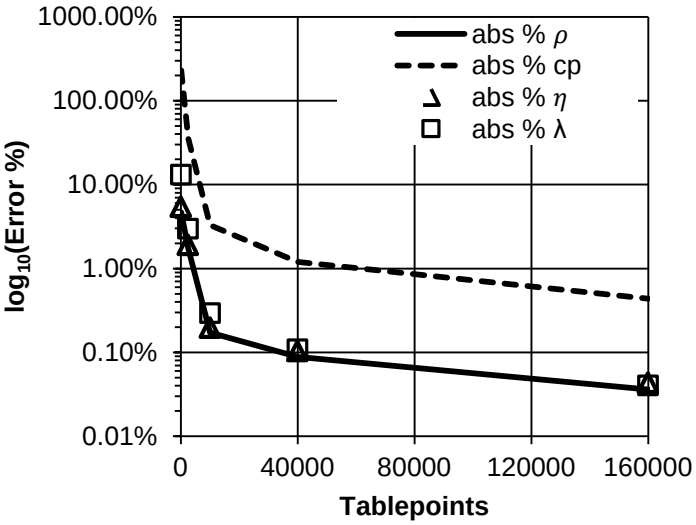

Figure 2 – Reduction of the error in property calculation with increasing table resolution

Aerodynamics of sCO2_HeRo_CC_1002

The compressor based on the parameters given in chapter “Design” is a starting point for the further investigations. Besides the parameters at impeller inlet and outlet, further quantities are required.

Figure 3 shows the cross-section on the left hand side and the meridional contour of the impeller on the right hand side. The semi-open impeller has 22 blades (n_{Blade}). Up to 50 % stream wise position the mean line of the blades is straight or in other words the blades are not curved. Between 50 % and 100 % the blade angle changes linearly to an outlet angle of 90°. The meridional contour shown on the right hand side is constructed with the constraint that the stage flow coefficient defined by Eq. 3 is equal at the inlet and at the outlet. The impeller side walls – hub and shroud – rotate together with the

blades. The diffusor side walls and inlet side walls are in the stationary system. At the inlet, the total pressure p_{tot} = 78.3 bar and the total temperature T_{tot} = 33 °C are specified as boundary conditions for the CFD simulations. The mass flow rate $\dot{m}$ = 0.65/n_{Blade} kg/s is specified as the outlet boundary condition. To find out the impact of the fluid parameters two different sets of CFD-simulations are performed. In the first simulation, the real fluid properties are taken into account and in the second simulation, constant properties are used. The constant properties are derived from the real fluid property calculations computing the average of ρ, c_p, λ, η from the values at the inlet and outlet.

$$\varphi_{Stage} = \frac{c_m}{u_2} \tag{3}$$

Figure 4 shows the static pressure along the stream wise coordinate *S* as area averaged quantity. The inflow section is located between *S* = 0 and *S* = 1; the impeller between *S* = 1 and *S* = 2 and the diffusor between *S* = 2 and *S* = 3. Results obtained by considering real fluid properties are highlighted with circles and the ones calculated with constant fluid properties are shown by the bold black line. Only very narrow differences can be observed from this figure. Figure 5 depicts the blade loading at 50 % blade height. Results obtained by considering real fluid properties are again highlighted with circles and the ones calculated with constant fluid properties are again visualized by the bold black line. Only a little variation of the pressure is displayed comparing both simulations. Therefore, no indication for the necessity to use real fluid properties for the design procedure can be derived from these results.

This perception is in a complete contrast to what is expected viewing the course of density ρ and isobaric heat capacity c_p along the stream wise location *S* as shown in Fig. 6 and Fig. 7. Similar to the previous figures bold lines show results obtained with constant fluid properties and circles show results obtained with real fluid properties. The density varies between S=0 and S=3 by 14 %. The change in heat capacity is more significant, as it varies by a factor of eight, even though it is not observable in the pressure distribution around the blades. Basically two reasons can be identified for this unexpected behavior. On the one hand, even if c_p changes dramatically the value is quite high everywhere in the flow region. As a result, the temperature does not vary very much for a certain enthalpy change. Hence, the influence of the small temperature variation on the density is likewise small, resulting in a limited effect on the pressure. On the other hand, the Mach number *Ma* in the local frame of reference is below 0.3 as can be taken from Fig. 8. Most textbooks state that, if the *Mach number is less than* 0.3, even the calculation of compressible flow can be performed by incompressible methods without making big mistakes. In such a case, the coupling of the energy equation to the continuity and momentum equations can be neglected. Therefore, the influence of c_p is negligible.

Based on the CFD calculation conducted with real fluid properties an isentropic efficiency of 76.21 % is obtained for the compressor. This value is slightly higher than expected because the tip flow is not taken into account for the simulation. With a tip clearance of 0.4 mm an isentropic static efficiency of 65.53 % is determined.

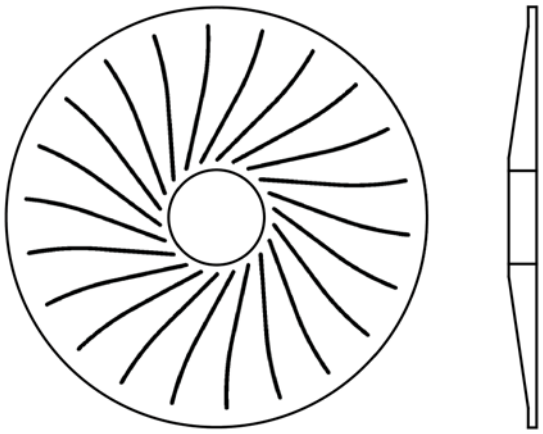

z-axis normal section **meridional-view**

Figure 3 – Geometry of the impeller blade including dimensions

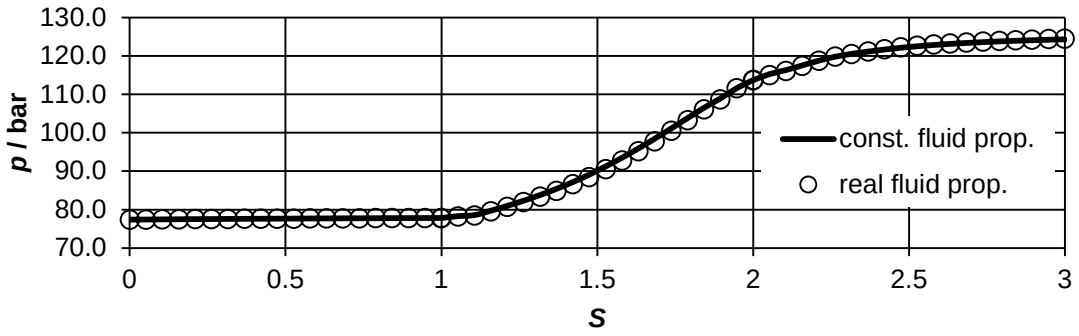

Figure 4 – Inlet to outlet static pressure course with constant fluid properties and real fluid properties

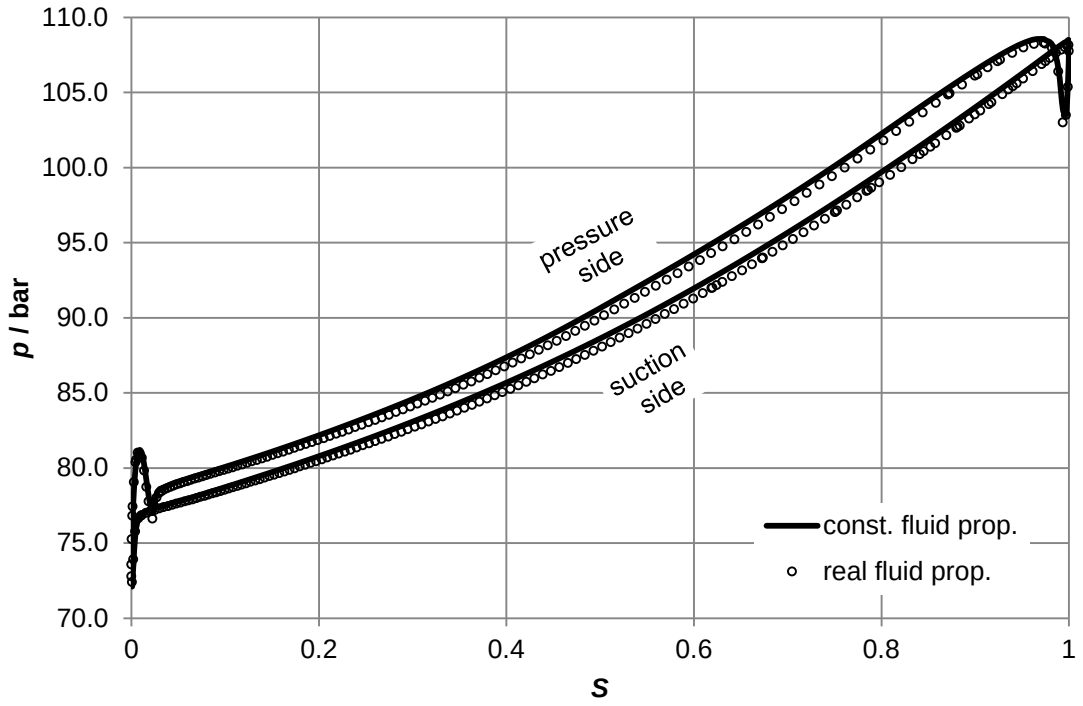

Figure 5 – Blade loading with constant fluid properties and real fluid properties

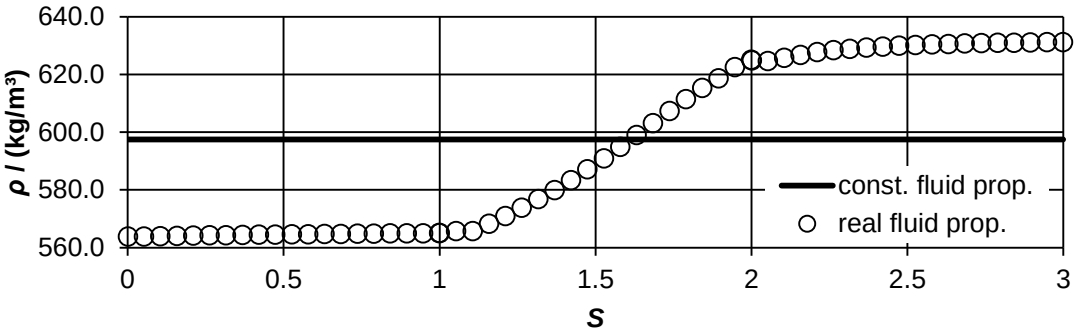

Figure 6 – Inlet to outlet density course with constant fluid properties and real fluid properties

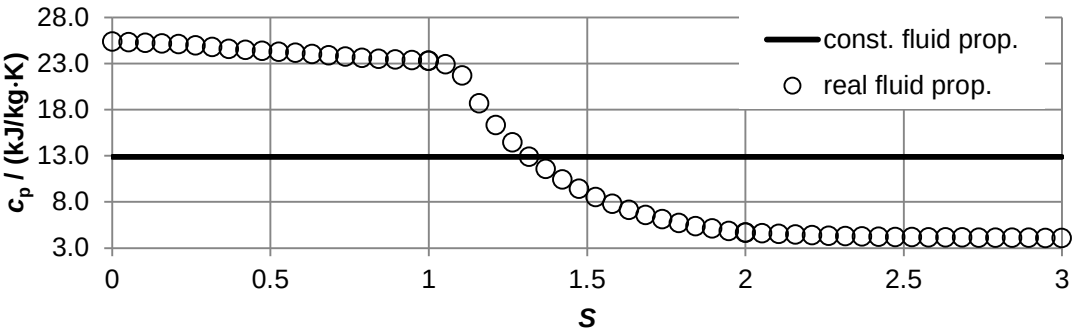

Figure 7 – Inlet to outlet c_p with constant fluid properties and real fluid properties

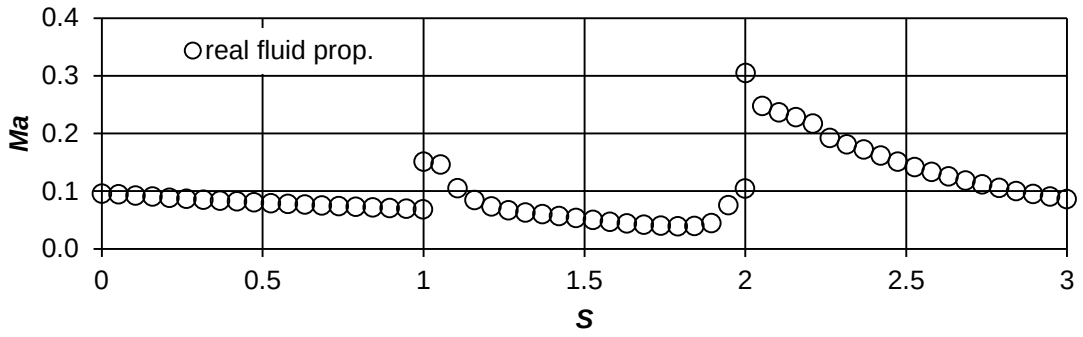

Figure 8 – Calculated Mach number

Summary and Conclusion

A first design of the compressor for the sCO2-HeRo is presented in this paper. Real fluid properties are implemented in the used CFD code and a satisfactory agreement between the values calculated during the simulation and the values directly computed from the equation of state is found.

An initial impeller and blade design is determined based on fundamental considerations at the impeller inlet and the impeller outlet. Constant blade thickness and relatively simple blade angle distribution is applied in order to perform the investigations.

The calculated compressor efficiency is acceptable for the scope of the sCO2-HeRo project particularly as no optimization is performed yet.

The influence of the real fluid properties on the calculation of the flow field in the compressor is negligible.

Acknowledgment

This project has received funding from the European research and training programme 2014 – 2018 under grant agreement No 662116.

References

Aungier, R. Centrifugal Compressors, 2000, pp. 8, Figure 1-9

Benra F.-K. , Brillert D. , Frybort O. , Hajek P. , Rohde M., Schuster S., Seewald M., Starflinger J., A supercritical CO2 low temperature Brayton-cycle for residual heat removal, submitted to the The 5th International Symposium - Supercritical CO2 Power Cycles March 28-31, 2016, San Antonio, Texas. 2016

Kretzschmar H.-J., Stoecker I., Property Library for Humid Gas Mixtures, 2014

Menter, F.R. Two-equation eddy-viscosity turbulence models for engineering applications. AIAA Journal. 1994, Vol. 32, 8.
Venker, J. A passive heat removal retrofit for BWRs. Nuclear Engineering International. 2013, Vol. 58, 711, 14 - 17.
Venker, J. et al., Transient Analysis of an Autarkic Heat Removal System. Proceedings of ICAPP 2014. 2014